Supplement of Atmos. Chem. Phys., 22, 1495–1514, 2022
https://doi.org/10.5194/acp-22-1495-2022-supplement
© Author(s) 2022. CC BY 4.0 License.

Atmospheric Chemistry and Physics
Open Access
EGU

Supplement of

Single-particle characterization of polycyclic aromatic hydrocarbons in background air in northern Europe

Johannes Passig et al.

Correspondence to: Johannes Passig (johannes.passig@uni-rostock.de)

The copyright of individual parts of the supplement might differ from the article licence.

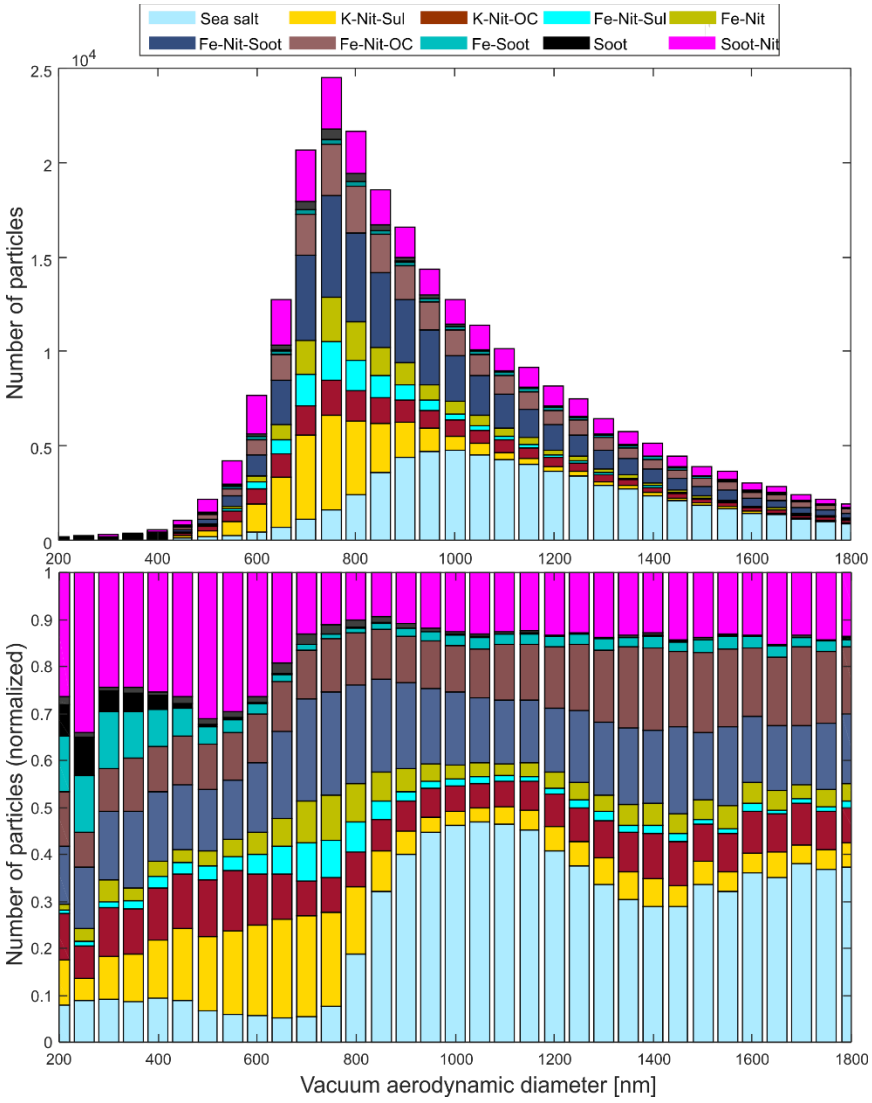

Fig. S1: Vacuum aerodynamic diameter of the general particle classes with respect to LDI mass spectra.

Fig. S2 (below): HYSPLIT back trajectories for 24 h run time, ending at the measurement site.

NOAA HYSPLIT MODEL
Backward trajectories ending at 0000 UTC 13 Oct 19
GFSQ Meteorological Data

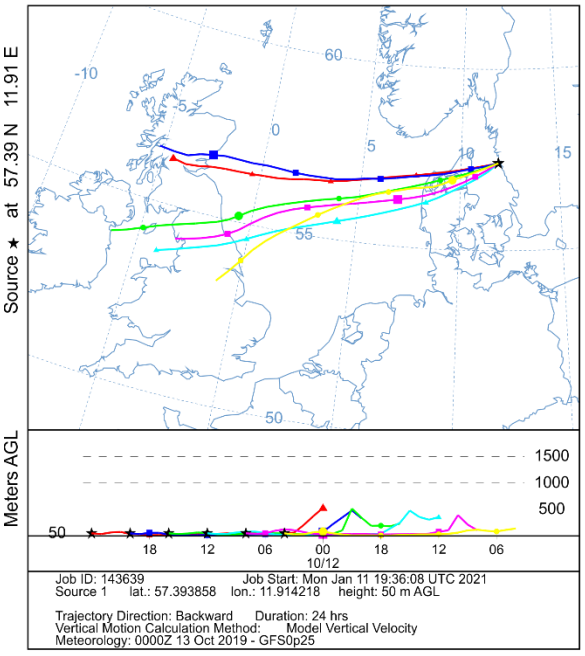

Job ID: 143639 Job Start: Mon Jan 11 19:36:08 UTC 2021
Source 1 lat.: 57.393858 lon.: 11.914218 height: 50 m AGL

Trajectory Direction: Backward Duration: 24 hrs
Vertical Motion Calculation Method: Model Vertical Velocity
Meteorology: 0000Z 13 Oct 2019 - GFS0p25

NOAA HYSPLIT MODEL
Backward trajectories ending at 0000 UTC 14 Oct 19
GFSQ Meteorological Data

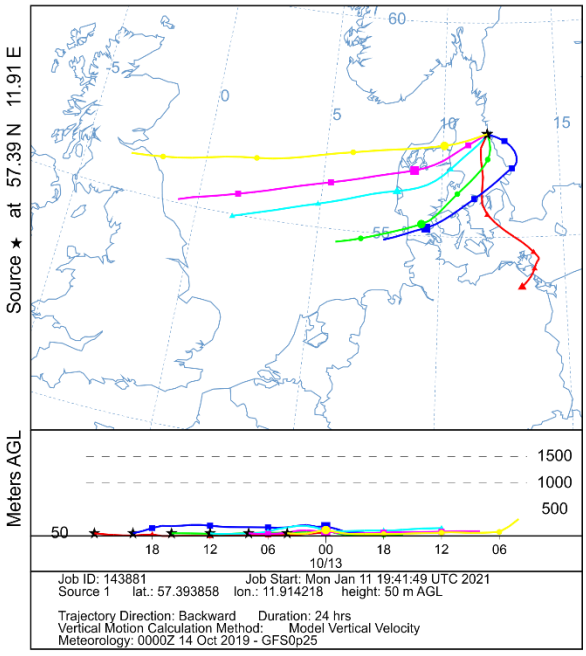

Job ID: 143881 Job Start: Mon Jan 11 19:41:49 UTC 2021
Source 1 lat.: 57.393858 lon.: 11.914218 height: 50 m AGL

Trajectory Direction: Backward Duration: 24 hrs
Vertical Motion Calculation Method: Model Vertical Velocity
Meteorology: 0000Z 14 Oct 2019 - GFS0p25

NOAA HYSPLIT MODEL
Backward trajectories ending at 0000 UTC 15 Oct 19
GFSQ Meteorological Data

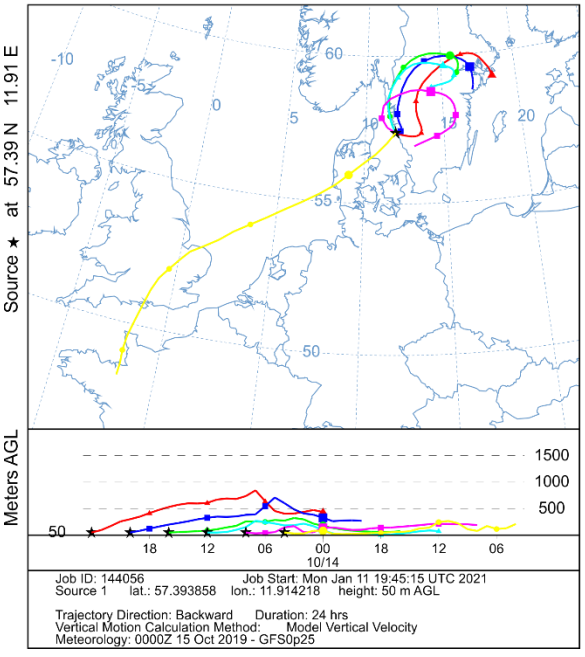

Job ID: 144056 Job Start: Mon Jan 11 19:45:15 UTC 2021
Source 1 lat.: 57.393858 lon.: 11.914218 height: 50 m AGL

Trajectory Direction: Backward Duration: 24 hrs
Vertical Motion Calculation Method: Model Vertical Velocity
Meteorology: 0000Z 15 Oct 2019 - GFS0p25

NOAA HYSPLIT MODEL
Backward trajectories ending at 0000 UTC 16 Oct 19
GFSQ Meteorological Data

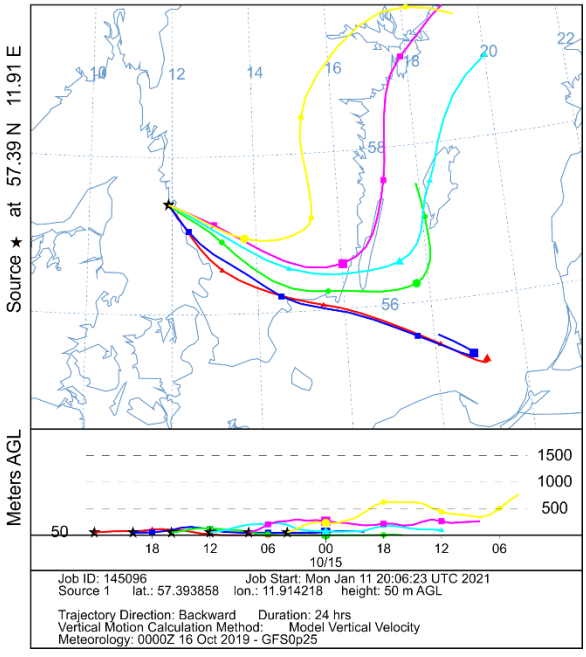

Job ID: 145096 Job Start: Mon Jan 11 20:06:23 UTC 2021
Source 1 lat.: 57.393858 lon.: 11.914218 height: 50 m AGL

Trajectory Direction: Backward Duration: 24 hrs
Vertical Motion Calculation Method: Model Vertical Velocity
Meteorology: 0000Z 16 Oct 2019 - GFS0p25

NOAA HYSPLIT MODEL
Backward trajectories ending at 0000 UTC 17 Oct 19
GFSQ Meteorological Data

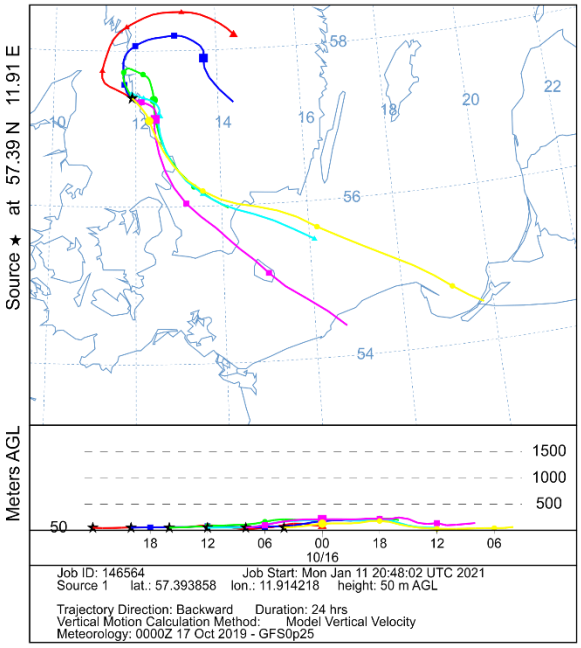

Job ID: 146564 Job Start: Mon Jan 11 20:48:02 UTC 2021
Source 1 lat.: 57.393858 lon.: 11.914218 height: 50 m AGL

Trajectory Direction: Backward Duration: 24 hrs
Vertical Motion Calculation Method: Model Vertical Velocity
Meteorology: 0000Z 17 Oct 2019 - GFS0p25

NOAA HYSPLIT MODEL
Backward trajectories ending at 0000 UTC 18 Oct 19
GFSQ Meteorological Data

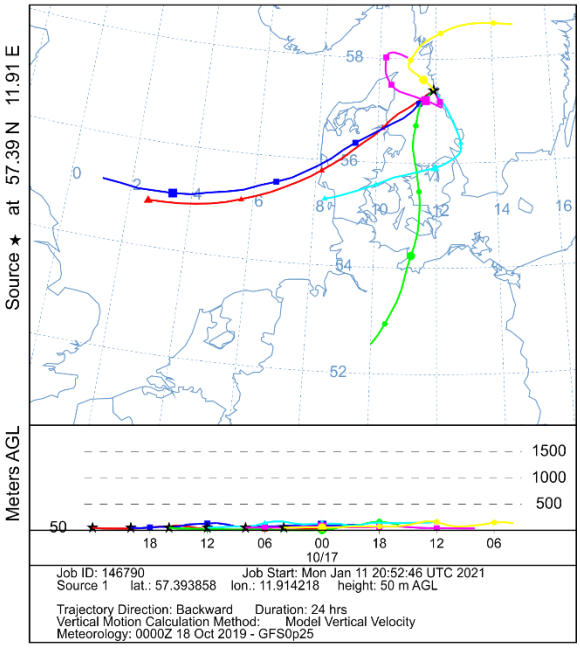

Job ID: 146790 Job Start: Mon Jan 11 20:52:46 UTC 2021
Source 1 lat.: 57.393858 lon.: 11.914218 height: 50 m AGL

Trajectory Direction: Backward Duration: 24 hrs
Vertical Motion Calculation Method: Model Vertical Velocity
Meteorology: 0000Z 18 Oct 2019 - GFS0p25

NOAA HYSPLIT MODEL
Backward trajectories ending at 0000 UTC 19 Oct 19
GFSQ Meteorological Data

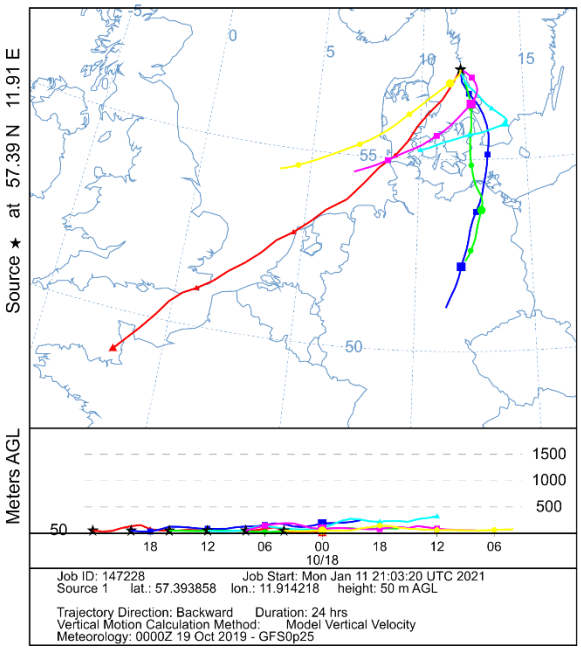

Job ID: 147228 Job Start: Mon Jan 11 21:03:20 UTC 2021
Source 1 lat.: 57.393858 lon.: 11.914218 height: 50 m AGL

Trajectory Direction: Backward Duration: 24 hrs
Vertical Motion Calculation Method: Model Vertical Velocity
Meteorology: 0000Z 19 Oct 2019 - GFS0p25

NOAA HYSPLIT MODEL
Backward trajectories ending at 0000 UTC 20 Oct 19
GFSQ Meteorological Data

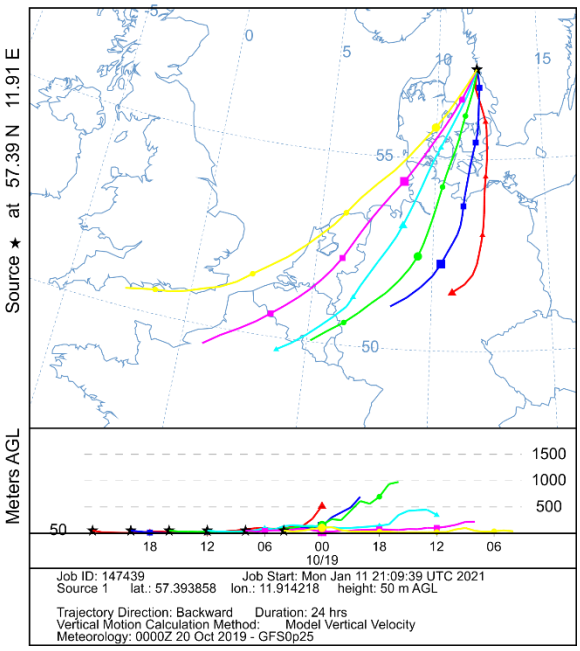

Job ID: 147439 Job Start: Mon Jan 11 21:09:39 UTC 2021
Source 1 lat.: 57.393858 lon.: 11.914218 height: 50 m AGL

Trajectory Direction: Backward Duration: 24 hrs
Vertical Motion Calculation Method: Model Vertical Velocity
Meteorology: 0000Z 20 Oct 2019 - GFS0p25

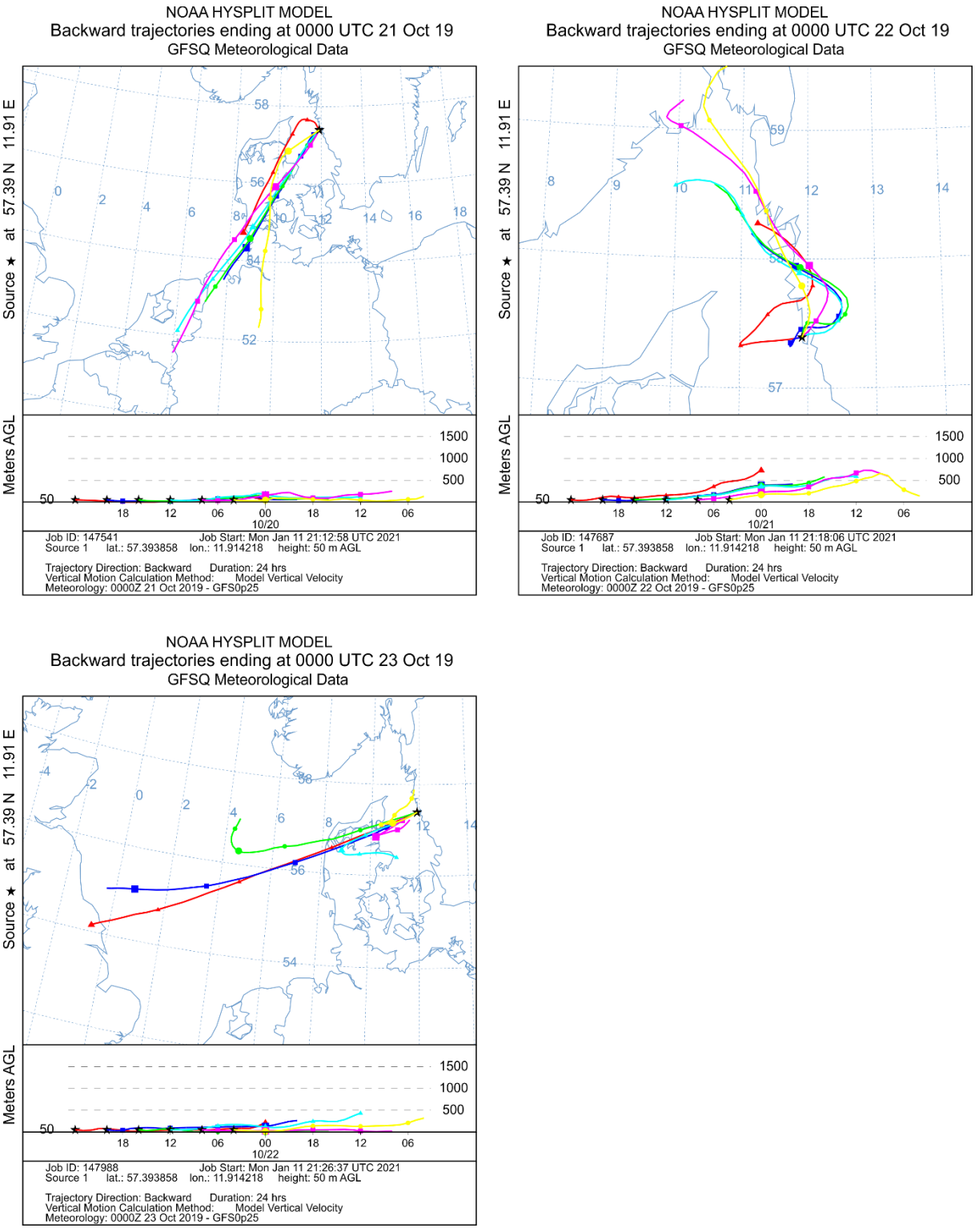

Fig. S2: HYSPLIT back trajectories for 24 h run time, ending at the measurement site.

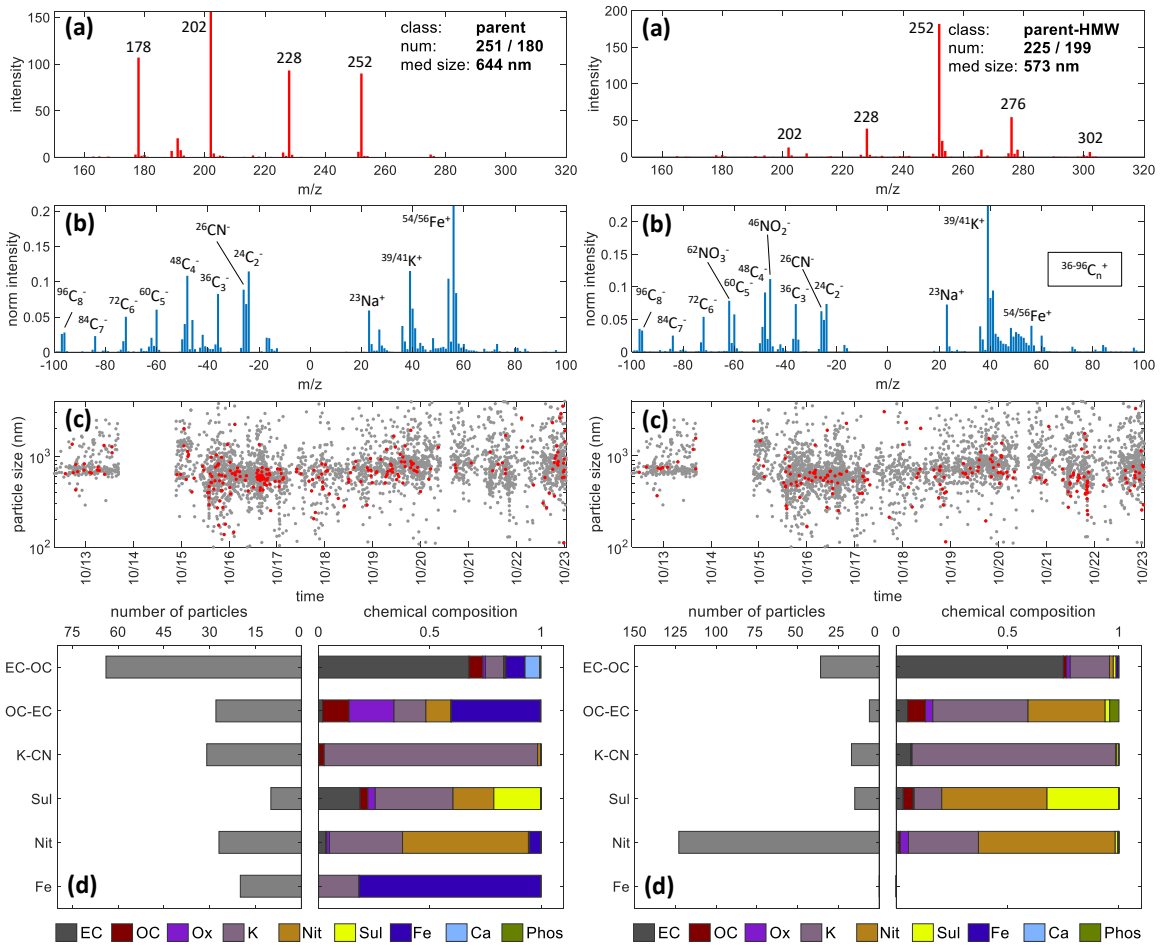

Fig. S3: Particles with signatures of only 'parent' PAHs show secondary nitrate more frequently than the "common" type (manuscript, Fig. 5), possibly as a result of PAH degradation by atmospheric ageing. (For figure explanation, see Fig. 5.)

Fig. S4: Additional 'parent' PAH peaks at high masses can result from wood combustion, but the further increased nitrate and sulfate signals could also be indicative for an advanced stage of ageing. (For figure explanation, see Fig. 5.)

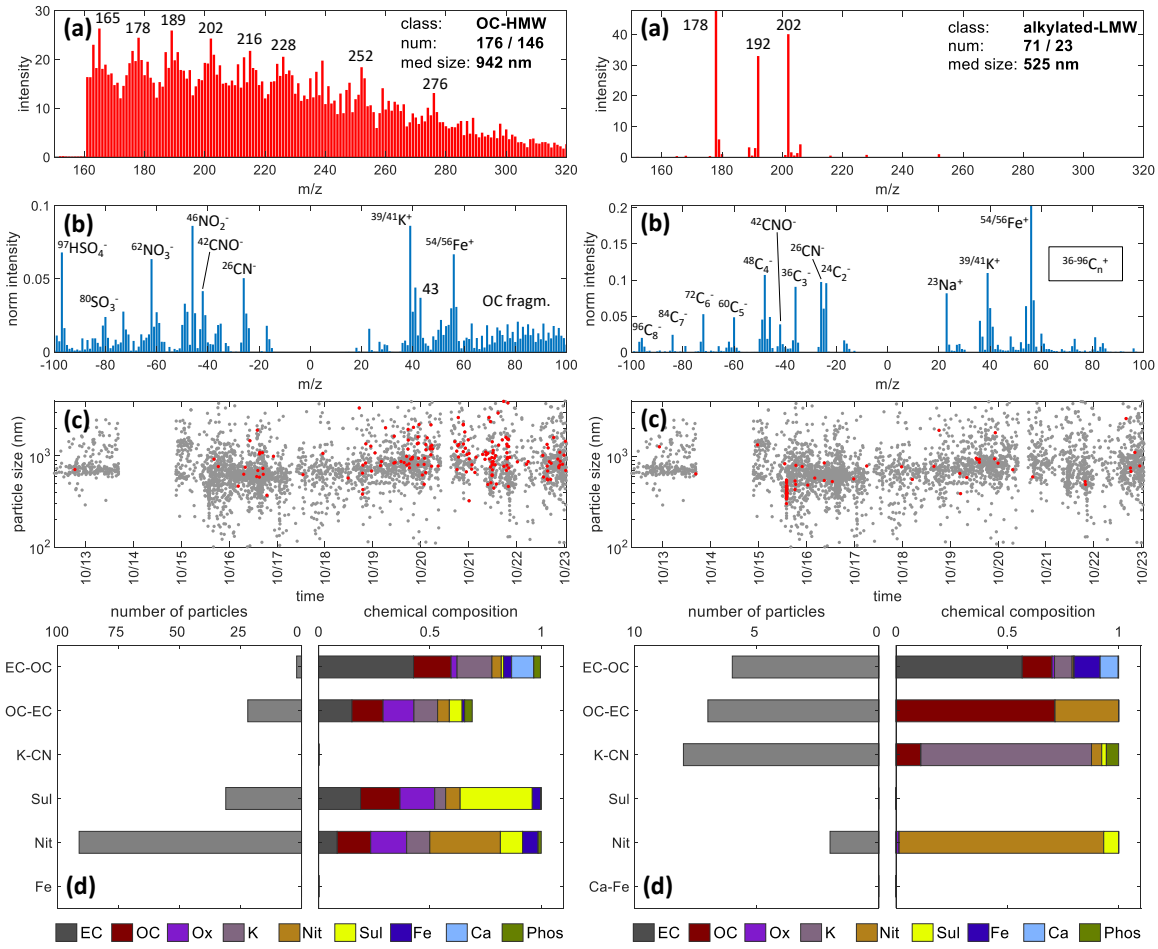

Fig. S5: Rows of high-mass OC peaks dominating are frequently associated with strong sulfate signals in addition to the nitrate, indicating enhanced SOA and oligomer formation by particle acidity. (For figure explanation, see Fig. 5.)

Fig. S6: Particles with strong signals from alkylated PAHs of low molecular weight could be attributed to a green waste burning fire at the 15th of October. (For figure explanation, see Fig. 5.)

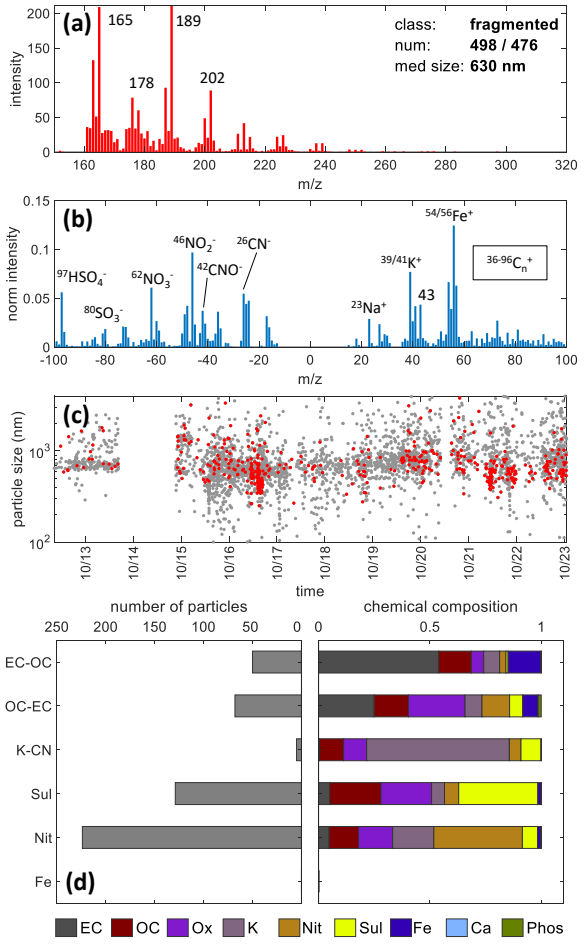

Fig. S7: Some particles show a characteristic fragment pattern with additional peaks at -2 m/z for each PAH signal and strong signals from secondary nitrate and sulfate. They could so far not be associated with a specific source or atmospheric process. (For figure explanation, see Fig. 5.)

Tab. S1: Assignment of the top-300 clusters of the ART-2a analysis of LDI mass spectra to main particle classes. The cluster spectra and temporal behavior are given in Fig. S8.

Sea salt	K-Nit-Sul	K-Nit-OC	Fe-Nit-Sul	Fe-Nit	Fe-Nit-Soot	Fe-Nit-OC	Fe-Soot	Soot	Soot-Nit
1	2	16	36	10	27	43	62	220	192
3	4	26	37	11	28	53	149		200
5	14	69	40	12	39	67	155		204
6	19	105	70	18	44	68	165		234
7	25	131	73	24	47	77	176		258
8	34	133	124	29	49	83	178		263
9	104	141	125	48	50	84	197		278
13	114	161	127	74	51	85	231		
15	119	175	147	86	52	90			
17	170	181	151	138	55	96			
20	174	186	158	139	58	97			
21	177	193	187	236	60	101			
22	182	199	209	238	66	106			
23	189	206	288		75	109			
30	190	212			76	110			
31	191	228			78	111			
32	194	233			79	112			
33	195	240			80	113			
35	202	245			81	117			
38	205	247			88	121			
41	207	248			89	122			
42	224	249			91	126			
45	229	251			92	128			
46	230	253			94	130			
54	250	262			95	132			

56	252	265			98	148			
57	254	270			99	150			
59	255	271			100	152			
61	256	272			103	153			
63	257	275			107	154			
64	264	280			108	157			
65	282	281			115	164			
71	290	286			116	166			
72	293	287			118	172			
82	295	291			120	179			
87	299	292			129	198			
93		300			134	221			
102					136	223			
123					140	232			
135					144	235			
137					145	259			
142					146	261			
143					156	266			
160					159	273			
163					162	284			
169					167				
171					168				
180					173				
183					208				
184					213				
185					214				
188					217				
196					218				
201					219				
210					222				
211					237				
215					237				
225					239				
226					242				
227					243				
241					244				
246					260				
267					269				
268					276				
274					277				
283					279				
289					294				
298					296				
					297				

Tab. S2: Assignment of the top-300 clusters of the ART-2a analysis of REMPI mass spectra to main (PAH) particle classes. The cluster spectra and temporal behavior are given in Fig. S9. The missing clusters reveal high-mass signatures of inorganic compounds (e.g. Pb^+, $K_3PO_4^+$ etc.) but no PAHs.

Common	PAH-HMW	Parent	Parent-HMW	PAH-OC-LMW	PAH-OC-HMW	OC-HMW	Alkylated	Alkylated-LMW	Fragmented
12	54	41	36	23	38	35	63	49	46
15	76	43	92	28		39	67		55
19	108	81	107	32			85		57
24	158	90	155	34			180		60
31			165	42					72
37			176	45					79
40			177	53					109
47									110
48									111
68									121
69									123
70									
82									
118									
119									
122									
157									
173									